Nuclear Instruments and Methods in Physics Research B 115 (1996) 246–250

NIM B
Beam Interactions with Materials & Atoms

Kinetic energy distributions of secondary molecular ions from thin organic films under ion bombardment

A. Delcorte *, P. Bertrand

Université Catholique de Louvain, PCPM, 1 Place Croix du Sud, B-1348 Louvain-la-Neuve, Belgium

Abstract

Langmuir–Blodgett films of tricosenoic acid deposited on gold have been bombarded by Ga^+ and Cs^+ ions and secondary ion mass spectra were measured by a Time-of-Flight spectrometer. The energy distributions of atomic ions are found to follow the Sigmund–Thompson law whereas, for the molecular C_xH_y positive and negative ions, the energy distributions have a much more intriguing structure. Within a given C_iH_y cluster, the energy distributions become broader for the ions that are more unsaturated. This effect is more important for the smaller clusters. The more saturated ions which have a structure close to that of the original molecule have the thinner energy distributions and these are only slightly dependent of the fragment mass. The results are tentatively interpreted on the basis of the chemical and molecular structure of the fragments as compared to that of the original hydrocarbon chains.

1. Introduction

Amongst the secondary ion properties, the kinetic energy distribution (KED) is of particular interest as it gives a direct insight into the energy transfer processes governing the emission. Although the study of the KED of secondary atomic and cluster ions has played a great role in the modelization of the emission process in keV bombardment of inorganic targets [1–7], the literature in which the KED of organic secondary ions are reported is less exhaustive [8–10] and rare are the cases where they are used for modelization [11,12]. Most of the models describing the emission process from inorganic targets are based on uncorrelated collision events that may be valid in the case of organic targets too. However, it is hard to believe that these models may explain every experimental data related to organic surfaces. Indeed, the ejection of the parent-like ions $(M+H)^+$, $(M-H)^-$ may unlikely be the result of a single or multiple collision with cascade atoms in uncorrelated motion as it may be the case for atomic and small organic ions. These particular features require a completely different treatment assuming the correlated motion of several atoms [13–15]. The fact that this may be a consequence of nuclear stopping is not unreasonable [14].

On the other hand, the molecular structure of the material (including the nature, orientation and strength of the bonds), which is often neglected in the above theoretical models for simplification reasons, may play an important role in the emission process, as pointed out by MD simulations [16]. This last approach will give us the key for a realistic interpretation of our results.

In this study, tricosenoic acid has been chosen as organic target for several reasons: (1) its properties, including its ability to transfer as homogeneous organized layers, are well known; (2) its structure constitutes a good model of hydrocarbon chains, suggesting that the observations may be extended to a lot of organic systems including polymers; (3) its weak bonding to the substrate gold atoms gives the opportunity to measure parent ions energy spectrum.

2. Samples preparation

The sample substrates were realized by evaporating gold onto clean silicon wafers under vacuum. The solution of tricosenoic acid ($C_{22}H_{43}COOH$) was then sprayed on the water subphase and transferred as LB film onto the substrates owing to a Lauda 2 apparatus (20 N/m^2, 25°C). For the KED measurements, only two layers were deposited in order to avoid sample charging under ion bombardment.

3. Experimental setup

The KED measurements were performed in a Time-of-Flight SIMS microprobe-microscope (Charles Evans & assoc.) using (5 kHz) pulsed Ga^+ beam (15 kV, 400 pA

* Corresponding author. Tel. +32 10 47 3582, fax +32 10 47 3452, e-mail delcorte@pcpm.ucl.ac.be.

SSDI 0168-583X(95)01563-9

DC) and Cs^+ beam (11 kV, 200 pA DC) [17]. The angle between the source and the spectrometer axis (perpendicular to the surface) is $-35°$ for Ga^+ and $+42°$ for Cs^+. In order to avoid sample degradation, the primary beam is rastered onto a (100×100 μm) area, allowing to keep the total ion fluence below 10^{13} ions/cm^2 for a set of energy spectra covering ions across the whole accessible mass range. During the secondary ions extraction periods, a (3000-Δ) V potential is applied to the sample where Δ is adjustable in order to acquire a selected part of the KED. The departing secondary ions are accelerated and focused before to enter a field free drift region. They are then 270° deflected by three hemispherical electrostatic analyzers (ESA) before reaching the detector. At the first ESA (+90° with respect to the spectrometer axis), the energy distribution is converted into a spatial distribution. The ions are then energy selected by a slit of known width (100 μm corresponding to a passband of 1.5 eV) placed at the crossover following the first ESA. Indeed, in this point, the spatial distribution is influenced only by the energy and angular distributions of the particle, and not by the initial position of the particle on the sample surface. The acquisition of mass spectra for different sample voltages (Δ) allows the collection of a complete KED. The determination of the zero energy point (3000 + C) V in this configuration is not trivial. This is why we prefer to characterize the KEDs by their FWHM in the following rather than by the position of the maximum or by the coefficient of the exponential dependence (n).

4. Results and discussion

4.1. Ga primary ions

We have recorded the KED of some atomic ions under Ga^+, 15 keV bombardment. Fig. 1a shows the raw distributions of negative atomic ions coming from the substrate and from the acid layer. The experimental points are well described by a Sigmund–Thompson law [1,2], in agreement with a simple collisional mechanism. The FWHMs of the distributions of Au, O, C are respectively 4.4, 6.9 and 11.4 eV and the binding energies (E_b) given by the curve fitting 3.8, 5.5, and 8.6 eV. In the case of gold, there is a good agreement between E_b and the heat of sublimation (3.6–3.8 eV [18]), which is usually considered as a good approximation of the surface binding energy. In the case of carbon, E_b is of the order of the heat of sublimation of graphite (7.4 eV).

Table 1 displays the FWHM values for most of the positive organic secondary ions. The most striking effect concerns the C_xH_y ions. As shown in Fig. 1b, their KED shifts and broadens when the number y of hydrogen atoms decreases, e.g. the more saturated ions peak at a lower energy and their tail factor (n) is greater than the one of unsaturated ions (unsaturation effect). On the other hand,

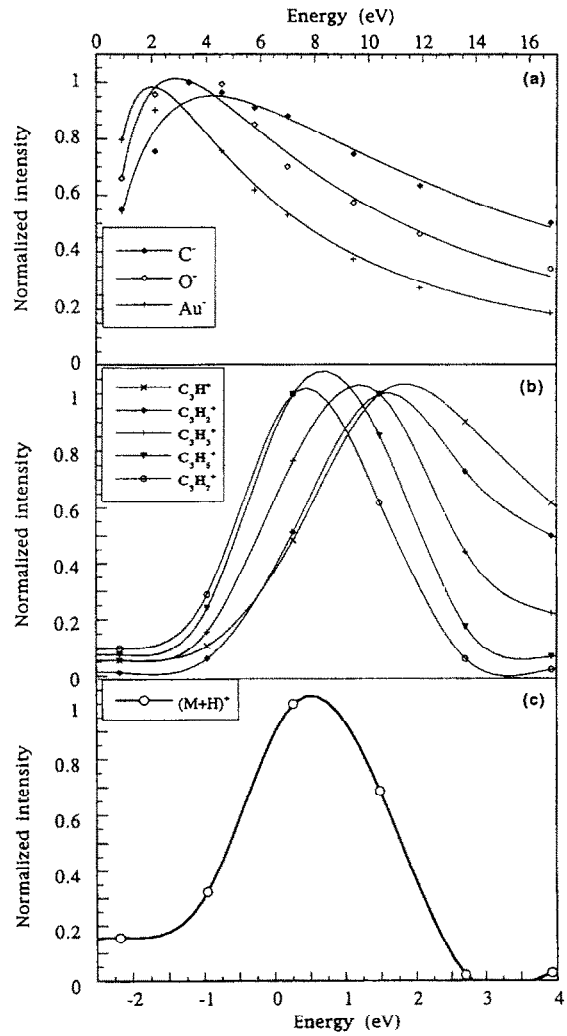

Fig. 1. (a) KED of atomic secondary ions (negative mode) coming from the substrate (Au) and from the acid layer (C, O). The full lines represent the Sigmund–Thompson fitting $\{Y(E) = CE/(E + E_b)^3\}$. (b) KED of the $C_xH_y^+$ ions ($x = 3$; $y = 1$, 2, 3, 5 and 7). (c) KED of the parent ion $(M + H)^+$. The zero energy corresponds to the fitting of the KED of the atomic secondary ions.

the spreading of the FWHMs within a C_iH_y series increases and the KED of equally saturated fragments (C/H constant) broadens when the number of carbon atoms (i) of the ion decreases (size effect). It seems that the regularity with which the unsaturation effect is occurring within the different C_iH_y series may be a very important clue for the interpretation of this result. In addition, the existing models are not able to reproduce the regular distribution broadening within the C_iH_y series, which is in favor of an interpretation based on the structure of the material. This point will be emphasized in the following. The KED of the parent-like ion $(M + H)^+$ is displayed in Fig. 1c. Though

the width of the slit may be a limiting factor here, the distribution is similar to the one of the most saturated ions.

Considering that the ionization processes may influence the KED of secondary ions, we may expect a distinct behavior for negative ions. Experiments with Ga^+, 15 keV show that it is not the case for the C_xH_y ions. In Fig. 2, we report the FWHMs of positive and negative ions as a function of their mass. The two sets of data merge together showing that the "unsaturation broadening" is observed whatever the ions polarity and suggesting moreover that the energy transfer mechanisms may be similar and little affected by the ionization processes. The distributions of the negative ions containing oxygen and reflecting the structure of the chain are very similar with a FWHM around 3 eV ($CHOO^-$, CH_3COO^-, $C_2H_3COO^-$, $C_{22}H_{43}O_2^-$, $C_{23}H_{41}O_2^-$, $C_{23}H_{43}O_2^-$).

4.2. Cs primary ions

In order to get a more general view of the emission process in this system, and particularly to evidence a possible asymmetry in the secondary ions angular distributions, the KEDs of the C_xH_y ions have been recorded under Cs^+, 11 keV bombardment. The different geometry of the Cs gun allows us to isolate the effect due to the angular distribution from that of the KED in the measured distributions. Indeed, at the energy slit position, the effect of the first ESA is to deflect the ion with an initial axial energy of an angle less than 90°, which is assumed only for ions emitted with zero kinetic energy along the spectrometer axis. An additional term of radial kinetic energy due to the angular distribution causes either an increase (> 90°) or a decrease of the deflection, thus interferring with the KED to be measured. Since Ga^+ and Cs^+ beam line are mounted in opposite direction with respect to the spectrometer axis, if an anisotropic angular distribution of the secondary ions oriented with respect to the primary beam leads to a relative broadening of the distribution in the Ga^+ bombardment configuration, it will result in a relative narrowing of the distribution in the Cs^+ bombardment configuration (see experimental setup).

The results for the Cs^+ bombardment are summarized in Table 1. For a given ion, the FWHM is in general greater for Cs^+ than for Ga^+ bombardment. This may be due to an angular effect affecting every secondary ions in the same way or to the nature of the primary beam itself. The differences of nuclear stopping power and lateral straggling of the primary ions [19] could account for an increase of the energy transmitted to the surface atoms and hence for a broader KED of the secondary ions in the Cs^+ mode. A slightly inhomogeneous surface potential can not be excluded too. Anyway, the broadening of the KED when the unsaturation of the ion increases is confirmed below mass 50 D, showing that the angular distribution is certainly not the reason of this effect in the low mass range.

4.3. Modelization of the C_xH_y ions behavior

On the basis of the structure of the target, we have developed a model explaining the C_xH_y behavior. In our approach, large fragments are emitted after a collision between an atom of the cascade and one of the carbon atoms belonging to the fragment precursor (by a mechanism which is not yet precised). The total energy transmitted to the departing fragment is then distributed as kinetic and internal energy. The internal energy fraction (vibration and rotation) is increasing with the fragment size [5]. In addition, we consider this internal energy as an excess energy able to lead to the rearrangement of the fragment if it is superior to the corresponding potential barrier for reorganization. From these hypotheses, we can draw two important consequences: (i) for a given impact energy, the greater is the departing fragment, the lower will be its kinetic energy (size effect) and (ii) for a given precursor fragment, the greater is the total energy transmitted, the greater will be the kinetic and the internal energies and the more important the reorganization, in agreement with Ref. [20] (reorganization effect).

In the case of tricosenoic acid, the single breaking of a C–C bond due to the collision with an atom of the cascade will produce a precursor C_xH_y where $y = 2x - 1$. If the total energy transmitted to the fragment is great enough, it will have an important kinetic energy and, in parallel, an excess of internal energy that may be sufficient to lead to reorganization by hydrogen elimination [21] (ii). The reorganized fragments, C_xH_{y-2}, will have a greater mean kinetic energy than the remaining C_xH_y ions, resulting from a softer collision. A very energetic initial collision will result in a more pronounced reorganization of the sputtered fragment. The general consequence will be valid for each C_xH_j cluster: the less saturated are the fragments,

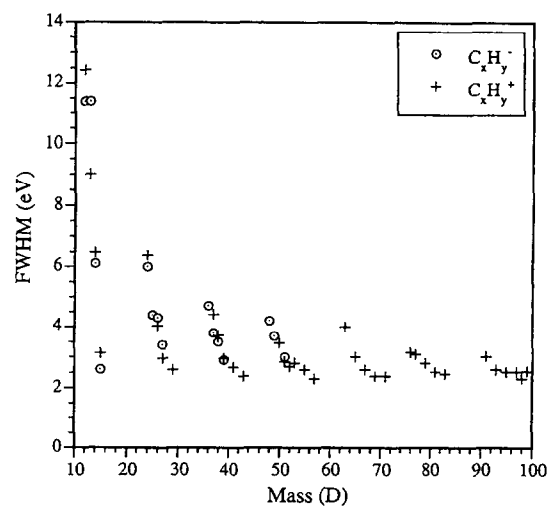

Fig. 2. FWHM of the distributions of the positive and negative C_xH_y ions as a function of their mass.

Table 1
FWHM of the distributions of the positive C_xH_y ions (Ga^+, 15 keV; Cs^+, 11 keV)

Ion formula	Mass (D)	FWHM [eV] (Ga^+)	FWHM [eV] (Cs^+)	Ion formula	Mass [D]	FWHM [eV] (Ga^+)	FWHM [eV] (Cs^+)
$C_xH_y^+$							
C^+	12	12.4		$C_5H_3^+$	63	4.0	3.9
CH^+	13	9.0		$C_5H_5^+$	65	3.0	3.5
CH_2^+	14	6.5		$C_5H_7^+$	67	2.6	3.1
CH_3^+	15	3.1	4.6	$C_5H_9^+$	69	2.4	3.0
				$C_5H_{11}^+$	71	2.4	
C_2^+	24	6.4					
$C_2H_2^+$	26	4.0	6.0	$C_6H_4^+$	76	3.2	
$C_2H_3^+$	27	2.9	3.7	$C_6H_5^+$	77	3.1	3.8
$C_2H_5^+$	29	2.6	3.1	$C_6H_7^+$	79	2.8	3.3
				$C_6H_9^+$	81	2.5	3.1
C_3H^+	37	4.4	5.9	$C_6H_{11}^+$	83	2.4	3.5
$C_3H_2^+$	38	3.7	4.9				
$C_3H_3^+$	39	2.9	3.8	$C_7H_7^+$	91	3.0	3.7
$C_3H_5^+$	41	2.7	3.1	$C_7H_9^+$	93	2.6	3.3
$C_3H_7^+$	43	2.4	2.9	$C_7H_{11}^+$	95	2.5	3.5
				$C_7H_{13}^+$	97	2.5	3.7
$C_4H_2^+$	50	3.5					
$C_4H_3^+$	51	2.8	3.1	$C_8H_7^+$	103		2.3
$C_4H_4^+$	52	2.7		$C_8H_9^+$	105		3.8
$C_4H_5^+$	53	2.8	3.4	$C_8H_{11}^+$	107		4.1
$C_4H_7^+$	55	2.6	3.1	$C_8H_{13}^+$	109	2.8	3.7
$C_4H_9^+$	57	2.3	3.8	$C_8H_{15}^+$	111	3.1	3.9
				$C_8H_{17}^+$	113		2.8
$C_xH_yO_z^+$							
CHO^+	29	3.2	4.2	$C_{23}H_{43}O^+$	335	2.4	3.2
CH_3O^+	31	2.8	3.3	$C_{23}H_{43}O_2^+$	351		3.2
$C_2H_3O^+$	43	3.1	3.0	$C_{23}H_{45}O_2^+$	353	2.4	
$C_2H_5O^+$	45	2.9	2.7				
$C_3H_5O^+$	59	2.4	3.1				

the greater will be their kinetic energy (unsaturation effect). Together with the effect of the size (i), this explains qualitatively the behavior of the C_xH_y ions. The quantitative details of the model will be given elsewhere [22].

5. Conclusion

The results are in agreement with a predominant effect of the chemical structure of the bombarded species on the kinetic energy distributions of the secondary molecular ions. The ions resembling the structure of the tricosenoic acid have indeed very narrow distributions whereas the less characteristic ones exhibit broader distributions. Our model, focusing on the structure of the bombarded hydrocarbon chains, helps to understand the rearrangement and fragmentation reactions affecting the C_xH_y ions. It suggests that hydrogen elimination may be an important mechanism for the deexcitation of the C_xH_y ions having an excess of internal energy. In order to interpret the kinetic energy distributions of secondary ions formed from organic samples, our work shows that the future theoretical developments will have to take into account the chemical and molecular structure of the target.

Acknowledgements

The authors wish to thank Dr. B. Schueler for helpful discussions concerning the experimental part as well as L. Langer and P. Hendlinger for the samples preparation. This work and A. Delcorte are supported by the "Action de Recherche Concertée" (94/99-173) of the "Communauté Française de Belgique, Direction Générale de l'Enseignement Supérieur et de la Recherche Scientifique". The ToF-SIMS equipment was acquired with the support of the "Région Wallonne" and "FRFC-Loterie Nationale" of Belgium.

References

[1] M.W. Thompson, Philos. Mag. 18 (1968) 377.
[2] P. Sigmund, in: Sputtering by Particle Bombardment I, ed. R. Behrisch (Springer, Berlin, 1981) p. 9.
[3] G. Blaise and G. Slodzian, Rev. Phys. Appl. 8 (1973) 105.
[4] M.A. Rudat and G.H. Morrison, Surf. Sci. 82 (1979) 549.
[5] H.M. Urbassek, Nucl. Instr. and Meth. B 18 (1987) 587.
[6] R. Hoogerbrugge and P.G. Kistemaker, Nucl. Instr. and Meth. B 21 (1987) 37.
[7] R.A. Haring, H.E. Rosendaal and P.C. Zalm, Nucl. Instr. and Meth. B 28 (1987) 205.
[8] L. Kelner and S.P. Markey, Int. J. Mass Spectrom. Ion Proc. 59 (1984) 157.
[9] L. Kelner and T.C. Patel, Springer Ser. Chem. Phys. SIMS V 44 (1986) 494.
[10] G.J.Q. van der Peyl, W.J. van der Zande, R. Hoogerbrugge and P.G. Kistemaker, Adv. Mass Spectrom. 10 (1986) 1511.
[11] G.M. Lancaster, F. Honda, Y. Fukuda, J.W. Rabalais, J. Am. Chem. Soc. 101 (1979) 1951.
[12] R. Hoogerbrugge and P.G. Kistemaker, Nucl. Instr. and Meth. B 18 (1987) 600.
[13] B.U.R. Sundqvist, Nucl. Instr. and Meth. B 48 (1990) 517.
[14] I.S. Bitensky, Nucl. Ins. Meth. B 83 (1993) 110.
[15] W. Ens, B.U.R. Sundqvist, P. Hakansson, D. Fenyö, A. Hedin and G. Jonsson, J. Phys. (Paris) C 2 (1989) 9.
[16] R.S. Taylor, C.L. Brummel, N. Winograd, B.J. Garrison and J.C. Vickerman, Chem. Phys. Lett. 233 (1995) 575.
[17] B.W. Schueler, Microsc. Microanal. Microstruct. 3 (1992) 119.
[18] R.C. Weast, ed., Handbook of Chemistry and Physics, 61st ed. (Chemical Rubber Co., Florida, 1981).
[19] J.P. Biersack, in: Ion Beam Modification of Insulators, eds. P. Mazzoldi and G.W. Arnold (Elsevier, Amsterdam, 1987).
[20] A. Benninghoven, in: Ion Formation from Organic Solids, ed. A. Benninghoven (Springer, Berlin, 1982) p. 77.
[21] A. Delcorte, L.T. Weng and P. Bertrand, Nucl. Instr. and Meth. B 100 (1995) 213.
[22] A. Delcorte and P. Bertrand, Nucl. Instr. and Meth. B, to be published.